The dilute Potts model on fractal lattices

1991 J. Phys.: Condens. Matter 3 1727

(http://iopscience.iop.org/0953-8984/3/12/004)

J. Phys.: Condens. Matter 3 (1991) 1727–1739. Printed in the UK

The dilute Potts model on fractal lattices

A Bakchich†, A Benyousseff† and N Boccara‡§

† Laboratoire de Magnétisme, Faculté des Sciences, BP 1014, Rabat, Morocco

‡ DPh-G, PSRM, Institut de Recherche Fondamentale, Centre d'Etudes Nucléaires, Saclay, 91191, Gif-sur-Yvette Cédex, France

§ Department of Physics, Box 4348, University of Illinois, Chicago, IL 60680, USA

Received 17 July 1989, in final form 23 August 1990

Abstract. We study the critical properties of the randomly bond-diluted q-state Potts ferromagnetic and antiferromagnetic models for a family of infinitely ramified exact fractals. Within Migdal's approximation we investigate the influence of bond dilution on the phase diagrams, and we calculate the dependence of the critical exponents upon fractal geometries.

1. Introduction

In recent years, much interest has been devoted to the study of phase transitions on fractal lattices. These have been studied using exact real-space renormalization group techniques (Nelson and Fisher 1975, Dhar 1977, Gefen *et al* 1980, Melrose 1983, Hu 1985), approximate renormalization schemes using bond moving (Gefen *et al* 1983, 1984, Riera and Chaves 1986, Hao and Yang 1987), and more recently with Monte Carlo techniques (Bhanot *et al* 1984, 1985, Bonnier *et al* 1987) and finite-size scaling theory (Dhar 1988). These studies showed that the critical properties of spin systems on fractals depend, apart from the fractal dimension D, on other geometrical parameters such as the connectivity Q and the lacunarity L that distinguish self-similar fractals from translationally invariant lattices with the same non-integer D. By translationally invariant lattices with the same non-integer D we mean the usual analytic continuation around a critical dimension, such as the continuous ε-expansions in the theory of critical phenomena (Wilson and Fisher 1972).

Works so far have focused on the critical behaviour of non-random systems for these fractals. A relatively small number of papers (Boccara and Havlin 1984) have been devoted to studying the influence of geometrical factors on the critical properties, for systems in the presence of bond inhomogeneity. It is our purpose to fill this gap. We exhibit some rather simple calculations to study the criticality associated with the quenched bond-diluted q-state Potts ferromagnet (FM) and antiferromagnet (AFM) on Sierpinski carpets. We investigate the influence of bond dilution on the phase diagrams and we calculate the dependence of the critical exponents upon fractal dimension and lacunarity, using an approximate real-space renormalization group method based on the Migdal-Kadanoff (MK) recursion relations (Migdal 1975, Kadanoff 1976). This problem has been studied extensively for regular Euclidean lattices and temperature–concentration phase diagrams have been calculated for these systems (Wu 1980). For

0953-8984/91/121727 + 13 $03.50

the family of fractals which will be described below we found similar phase diagrams, and the percolation behaviour is characterized by a bond percolation fixed point and its associated eigenvalue exponent whose variation with fractal geometries is similar to that of the critical temperature and thermal exponent, which was shown previously for the Ising and the Potts models.

The present work is organized as follows. In section 2 we describe the construction of fractal lattices and introduce the geometrical parameters (fractal dimension and lacunarity) characterizing these systems. Section 3 is devoted to an analysis of the Potts model on large-lacunarity carpet families. In section 4 we perform a renormalization group scheme which enables us to consider both large- and small-lacunarity carpets. We draw our final conclusions in section 5.

2. Construction of the fractal lattices

The fractal lattices studied in this paper are the Sierpinski carpets which are characterized, in addition to their non-integer fractal dimensionality D ($1 < D < 2$), by an infinite order of ramification which exhibits phase transitions at finite temperatures and non-trivial percolation thresholds. They are constructed by a subdivision of a unit square into b^2 subsquares, out of which l^2 squares are cut (b and l being integers, $l \leqslant b - 2$). This procedure is then repeated for the smaller squares and iterated until one obtains the fractal lattice in the limit of an infinite number of iterations. The fractal dimensionality D as a function of the scaling factor b is given by

$$D = \ln (b^2 - l^2)/\ln (b). \tag{2.1}$$

Thus the Sierpinski carpets are characterized by specific values of b and l. Letting b have a large value and varying l, one may construct carpets with D arbitrarily close to any value between 1 and 2.

In order to characterize the geometry of these fractals, one needs an additional parameter, the lacunarity L. Its intended function is to measure the extent of the failure of a fractal to be translationally invariant or the degree of homogeneity of a fractal. In the following, we shall be interested in cases in which the l^2 holes made at each step of construction of the fractal lattices are chosen in two ways, leading to geometries with different lacunarities: either they are condensed at the centre of the squares (corresponding to a large-lacunarity family), or they are distributed throughout each square (small-lacunarity family). Examples of these are presented in figures 1(a) and 1(b), respectively for $b = 7$ and $l = 3$ after two steps of the iterative procedure.

An approximate expression for the lacunarity of Sierpinski carpets was proposed by Gefen *et al* (1984):

$$L = \frac{1}{n(l)} \sum_i [n_i(l) - \bar{n}(l)]^2 \tag{2.2}$$

where

$$\bar{n}(l) = \frac{1}{n(l)} \sum_i n_i(l). \tag{2.3}$$

Here $n(l)$ is the total number of $l \times l$ cells contained in a square of $b \times b$ cells, and $n_i(l)$ the number of uneliminated cells for the ith $l \times l$ covering. This expression was improved

(Lin and Yang 1986, Wu and Hu 1987, Taguchi 1987, Wu 1988) to make its zero value a necessary and sufficient condition for a translationally invariant fractal, and to reflect the relative homogeneity of the carpets. Thus the following alternative expression for lacunarity was proposed (Wu and Hu 1987, Wu 1988):

$$L = \frac{1}{b-1}\sum_i L(s) \tag{2.4}$$

where

$$L(s) = \frac{1}{\bar{n}'(s)}\left(\frac{1}{n(s)}\sum_i [n_i(s) - \bar{n}'(s)]^2\right)^{1/2} \tag{2.5}$$

and

$$\bar{n}'(s) = s^2(b^2 - l^2)/b^2. \tag{2.6}$$

Since $(b^2 - l^2)/b^2$ is the fraction of uneliminated area, $\bar{n}'(s)$ provides a measure of uneliminated area in an $s \times s$ covering.

3. Recursion relations and results for large-lacunarity carpet families

Once the iterated procedure of lattice construction reaches a microscopic scale, we place at each site i of the fractal (including those which border the eliminated areas) a Potts variable which can be in any of q different states and is assumed to interact with its nearest neighbours. The appropriate Hamiltonian (in units of $1/\beta = k_B T$) is

$$-\beta H = \mp \sum_{\langle ij \rangle} K_{ij}(q\delta\sigma_i\sigma_j - 1) \tag{3.1}$$

where the + and − signs correspond to a FM and an AFM, respectively. The sum runs over all pairs of first-neighbour sites on the fractal, and K_{ij} is a random variable with the following probability distribution:

$$\mathcal{P}(K_{ij}) = (1-p)\delta(K_{ij}) + p\delta(K_{ij} - K) \qquad K > 0 \tag{3.2}$$

where p is the concentration of bonds and K the coupling of the pure system.

Before constructing the renormalization group recursive relations, let us associate with every bond characterized by an arbitrary coupling constant K_{ij}, a convenient variable defined as follows:

$$t_{ij} = [1 - \exp(\mp qK_{ij})]/[1 + (q-1)\exp(\mp qK_{ij})] = f(K_{ij}) \tag{3.3}$$

where the − and + signs correspond to a FM and an AFM, respectively. Note that the variable t is finite at both $K \to 0$ ($t = 0$) and $K \to \infty$ ($t = 1$ for a FM and $t = -1/(q-1)$ for an AFM).

The renormalization group equations are obtained using the usual *bond-moving* procedure which consists of first performing the decimation and then moving the bonds. Thus for a one-dimensional pure Potts model the exact recursion relation is

$$\tilde{t} = t^b \tag{3.4}$$

where $\tilde{t}$ is the renormalized interaction.

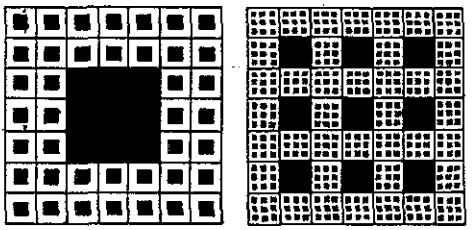

(*a*) (*b*)

Figure 1. Sierpinski carpet with $b = 7$, $l = 3$ after two steps of lattice construction: (*a*) holes condensed at the centre of the squares (large-lacunarity family); (*b*) holes distributed throughout the squares (small-lacunarity family).

For a two-dimensional square lattice the Migdal recursion relation is

$$t' = f[bf^{-1}(t^b)]. \tag{3.5}$$

For the fractal family described in figure 1(*a*) (large-lacunarity family) instead of having b paths we have only $b - l$ paths, and consequently the approximate Migdal relation is

$$t' = f[(b - l)f^{-1}(t^b)] \tag{3.6}$$

The recursion relation (3.6) has three fixed points: $t = 0$, $t = 1$ for a FM ($t = -1/(q - 1)$ for an AFM) and $t = t_c(b, l, q)$. The first two are stable and correspond to the infinite- and zero-temperature phases, respectively. The third is unstable and characterizes the paramagnetic-to-ferromagnetic (paramagnetic-to-antiferromagnetic) phase transition.

If the b interactions of each of the $b - l$ paths are random variables, the analogues of equation (3.6) determine each new local coupling $t'_{\alpha\beta}$ in terms of a set of original couplings $\{t_{ij}\}$:

$$t'_{\alpha\beta} = f\left[\sum_{i=1}^{b-l} f^{-1}\left(\prod_{j=1}^{b} t_{ij}\right)\right]. \tag{3.7}$$

If each t_{ij} is independently distributed according to the probability distribution $\mathcal{P}(t_{ij})$ given in (3.2), then the probability distribution $\mathcal{P}'(t'_{\alpha\beta})$ for the renormalized coupling is governed by

$$\mathcal{P}'(t'_{\alpha\beta}) = \int \prod_{\langle ij \rangle} \mathrm{d}t_{ij}\, \mathcal{P}(t_{ij}\delta[t'_{\alpha\beta} - t'_{\alpha\beta}(\{t_{ij}\})]. \tag{3.8}$$

Although initially the couplings are either present or absent corresponding to the two-peaked distribution (3.2), they do not remain so under iterations. A straightforward but tedious analysis of all the possible values for the interactions taking into account their respective probabilities gives the expression for the renormalized probability distribution $\mathcal{P}'(t'_{\alpha\beta})$ which is not of the same form as the initial one:

$$\mathcal{P}'(t'_{\alpha\beta}) = \sum_{m=0}^{b-l} C_m^{b-l}(p^b)^m(1 - p^b)^{b-l-m}\delta[t'_{\alpha\beta} - f(mf^{-1}(t^b))]. \tag{3.9}$$

To render the computations tractable we make an additional approximation at each

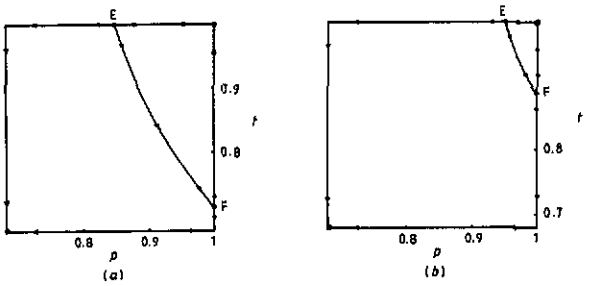

Figure 2. Phase diagrams in the (t, p)-space for the ferromagnetic Potts model on Sierpinski carpets: (*a*) $b = 3$, $l = 1$; (*b*) $b = 5$, $l = 3$.

iteration by forcing the transformed distribution to a two-peak form (Stinchcombe 1983):

$$\mathcal{P}'_{\text{approx}}(t'_{\alpha\beta}) = (1 - p')\delta(t'_{\alpha\beta}) + p'\delta(t'_{\alpha\beta} - t'). \tag{3.10}$$

Equating the zero and first moments of $\mathcal{P}'(t'_{\alpha\beta})$ and $\mathcal{P}'_{\text{approx}}(t'_{\alpha\beta})$ gives the recursion relations for the variables p and t within the two-peak approximation:

$$p' = 1 - (1 - p^b)^{b-l} \tag{3.11}$$

$$p't' = \sum_{m=0}^{b-l} C_m^{b-l}(p^b)^m(1 - p^b)^{b-l-m} f[mf^{-1}(t^b)]. \tag{3.12}$$

As usual for dilute systems the renormalized concentration p' given by (3.11) depends only upon the initial p but not on t. Therefore the linearization of the recursion relations (3.11) and (3.12) around the fixed points enables us to deduce the critical exponents through the relation

$$(\partial\mu'/\partial\mu)|_{\mu^*} = b^{y_\mu} \tag{3.13}$$

where μ can be t or p.

Thus the two derivatives that will be needed here are $\partial p'/\partial p$ and $\partial t'/\partial t$ which show explicitly the dependence of critical exponents upon the fractal dimensionality D. Indeed, for b fixed and varying l, which implies a variation in D, one obtains different critical exponents.

3.1. Results for ferromagnetic interactions

By iterating the renormalization group equations (3.11) and (3.12) in the (t, p) plane, one obtains the qualitative phase diagrams displayed in figure 2 for the following cases: in figure 2(*a*), $b = 3$, $l = 1$; in figure 2(*b*), $b = l + 2$, $l \neq 1$. In both cases the full curves EF represent the critical lines separating the disordered phase from the ordered phase. The critical point characterizing this transition is represented by the fixed point F, except at the $t = 1$ line which is characterized by the fixed point E. The (t, p) coordinates of the fixed points are

$$\text{E: } (1, p_c) \qquad \text{F: } (t_c, 1)$$

with the values t_c and p_c which are given in table 1 for each pair of b and l, and for several values of q. Note that, within the approximation described above, the recursion relations are close for a general number of Potts states but implicitly assume a second-order phase

Table 1. Results for the ferromagnetic Potts model on Sierpinski carpets with central cut-outs.

b	l	D	q	t_c	p_c	y_T	y_P
3	1	1.893	2	0.7861	0.8483	0.5619	0.4730
			3	0.7463	0.8483	0.6194	0.4730
			4	0.7172	0.8483	0.6617	0.4730
5	1	1.975	2	0.7511	0.8029	0.6707	0.5589
			3	0.7196	0.8029	0.7379	0.5589
			4	0.6969	0.8029	0.7858	0.5589
5	3	1.723	2	0.9210	0.9514	0.4139	0.3672
			3	0.8988	0.9514	0.4479	0.3672
			4	0.8813	0.9514	0.4747	0.3672
7	1	1.986	2	0.7772	0.8195	0.6828	0.5738
			3	0.7514	0.8195	0.7474	0.5738
			4	0.7329	0.8195	0.7930	0.5738
7	3	1.896	2	0.8406	0.8813	0.5942	0.5014
			3	0.8150	0.8813	0.6510	0.5014
			4	0.7963	0.8813	0.6919	0.5014
7	5	1.633	2	0.9594	0.9765	0.3491	0.3189
			3	0.9460	0.9765	0.3728	0.3189
			4	0.9348	0.9765	0.3921	0.3189

transition which is expected to hold for q less than or equal to a critical value q_c. For fractal lattices the q_c-values are unsolved. Therefore we show explicitly our results with $q = 2, 3, 4$. As we vary q, the above picture does not change, although the location of the critical line can change. Thus the qualitative phase diagrams are similar for any number of Potts states and in the particular case $q = 2$ we recover the results obtained by Boccara and Havlin for the Ising model.

Table 1 also shows the critical exponents y_T and y_P associated with the non-trivial fixed points for large-lacunarity carpet families. By inspection we note their variation with the fractal dimension. Indeed for b fixed and varying l, both ν_T and ν_P increase as D decreases, irrespective of the number of Potts states. If we had focused on the dependence of t_c and p_c upon D, we would have found the same variation. Thus the fractal dimension causes an effect on p_c and ν_P similar to that on t_c and ν_T, which was shown previously for the Ising and the Potts models. On the other hand, for a given lattice (b and l fixed), ν_T decreases as q increases, while ν_P remains constant.

3.2. Results for antiferromagnetic interactions

For the antiferromagnetic model, equation (3.12) exhibits a cut-off value $q_0(2 < q_0 < 3)$ above which there is only the paramagnetic phase, whereas for $q \leqslant q_0$ the system exhibits a low-temperature critical phase, as suggested for hypercubic lattices (Berker and Kadanoff 1980). As a consequence the AFM on fractal lattices has a phase transition only for $q = 2$. This result is consistent with the fact that, for $q \geqslant 3$, the ground state of the model has a non-zero entropy.

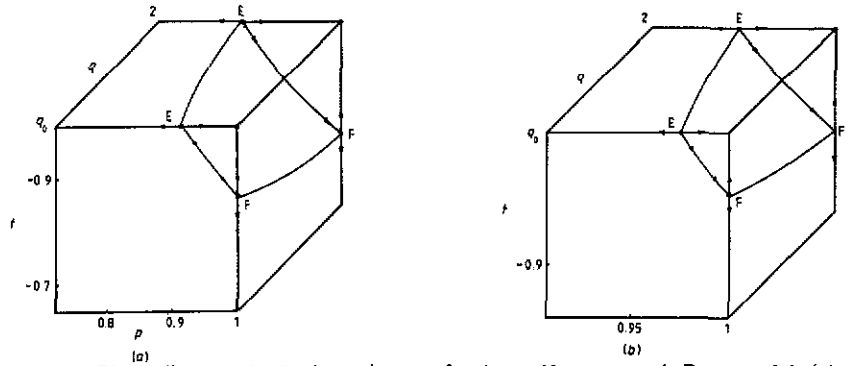

Figure 3. Phase diagrams in the (t, p, q)-space for the antiferromagnetic Potts model: (a) $b = 3, l = 1$; (b) $b = 5, l = 3$.

Table 2. Results for the antiferromagnetic Potts model on Sierpinski carpets with central cut-outs.

b	l	D	q	t_c	p^*	y_T	y_P
3	1	1.893	2	−0.7861	0.8483	0.5619	0.4730
5	1	1.975	2	−0.7511	0.8029	0.6707	0.5589
5	3	1.723	2	−0.9210	0.9514	0.4139	0.3672
7	1	1.986	2	−0.7772	0.8195	0.6828	0.5738
7	3	1.896	2	−0.8406	0.8813	0.5942	0.5014
7	5	1.633	2	−0.9594	0.9765	0.3491	0.3189

The phase diagrams in the (t, p, q)-space are shown in figure 3 for the following cases: in figure 3(a), $b = 3, l = 1$; in figure 3(b), $b = l + 2, l \neq 1$. The (t, p)-coordinates of the non-trivial fixed points are

$$\text{E: } (-1, p^*) \qquad \text{F: } (t_c, 1).$$

We find that the percolation threshold p^* at which the critical temperature goes to zero depends upon q. Indeed, for $q = 2$ (Ising model), p^* is equal to p_c which characterizes the bond percolation fixed point of the ferromagnet model while, for $2 < q \leq q_0$, p^* increases from p_c as q increases from 2. This result is similar to that obtained on regular Euclidean lattices (Wu 1980).

We summarize our numerical results in table 2, which shows the critical exponents around E and F for the antiferromagnetic Ising model. For each pair of b and l, characterizing various carpets, we calculate the critical exponents which depend explicitly on the fractal dimension as shown for the ferromagnetic model.

4. Recursion relations and results for large- and small-lacunarity carpet families

In order to establish the recursion relations for both large- and small-lacunarity carpet families, it is necessary to distinguish two sorts of nearest-neighbour bonds: those on the

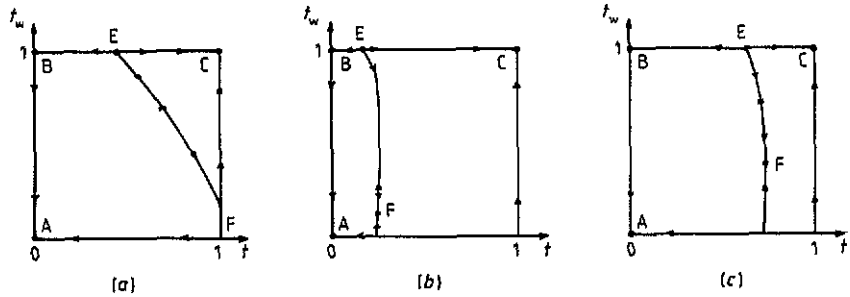

Figure 4. Phase diagrams for Sierpinski carpets with a central cut-out: (*a*) $b = 3$, $l = 1$; (*b*) $b = 7, l = 5$; (*c*) $b = 7, l = 3$.

boundary of a cut-out, K_w; internal bonds, K. For convenience we shall represent the recursive relations in terms of the appropriate variables t and t_w (defined by (3.3)) associated with bonds of strength K and K_w, respectively.

We specialize the following to the ferromagnetic model. When the system is homogeneous, the generalization of the recursion relations for the case in which a single large square, of size $l \times l$, is eliminated in the centre of each larger square (figure 1(*a*)) yields

$$t' = f[(b - l - 1)f^{-1}(t^b) + 2f^{-1}(t^{b-l}t_w^l) + (l - 1)f^{-1}(t^{b-l})] \tag{4.1}$$

$$t'_w = f\{f^{-1}(t_w^b) + [(b - l - 2)/2]f^{-1}(t^b) + f^{-1}(t^{b-l}t_w^l) + [(l - 1)/2]f^{-1}(t^{b-l})\}. \tag{4.2}$$

Note that within Migdal's approximation the recursion relations are within the two-dimensional parameter space (t, t_w). In the particular case $l = 0$ we recover the $d = 2$ results. The (t, t_w)-coordinates of the fixed points are

$$A: (0, 0) \qquad B: (0, 1) \qquad C: (1, 1) \qquad E: (t^E, 1) \qquad F: (t^F, t_w^F). \tag{4.3}$$

We find three distinct flow diagrams, in the (t, t_w)-space, as shown in figure 4. Figure 4(*a*) shows the special case $b = 3$, $l = 1$, which differs from all the cases with $b = l + 2 > 3$. Figures 4(*b*) and 4(*c*) correspond to $b = l + 2 = 7$ and $b > l + 2$ ($b = 7, l = 3$), respectively. As we vary q, the critical line is displaced but the overall picture is the same. Thus the qualitative phase diagrams obtained are similar for any number of Potts states.

In addition to this analysis, we iterated the recursion relations numerically and identified the locations of the fixed points E and F and their associated exponents. The numerical results are summarized in table 3. For each pair of b and l, and for several values of q (where the MK approximation predicts a second-order phase transition), the table lists D, t^E and the exponents near E, the coordinates of F and the exponents near F, and the critical value t_c at which the critical line crosses the diagonal ($t_c = t = t_w$).

A general result obtained from this calculation is the monotonic variation in the critical exponents and critical temperature with the fractal dimension, as shown in the previous section. One exception is the special case $b = 3$, $l = 1$, where the exponent associated with F does not obey the monotonic decreases with q.

If we had focused on small-lacunarity carpets, where the eliminated subsquares are uniformly distributed throughout each square (figure 1(*b*)), then we would have found, instead of (4.1) and (4.2), recursion relations of the following form:

$$t' = f[f^{-1}(t^b) + (b - 1)f^{-1}(t^{b-l}t_w^l)] \tag{4.4}$$

$$t'_w = f[f^{-1}(t_w^b) + (b - l - 1)f^{-1}(t^{b-l}t_w^l)]. \tag{4.5}$$

Table 3. Results for the Potts model on Sierpinski carpets with central cut-outs.

b	l	D	q	t^E	y_T^E	t^F	t_w^F	y_T^F	t_c
3	1	1.893	2	0.4354	0.5976	1	2.944×10^{-5}	0.9998	0.6827
			3	0.4027	0.6587	1	2.509×10^{-5}	0.9998	0.6414
			4	0.3795	0.7028	1	2.145×10^{-5}	0.9998	0.6119
7	3	1.896	2	0.6267	0.6015	0.7254	0.3865	0.5988	0.7013
			3	0.5976	0.6552	0.6977	0.3346	0.6497	0.6729
			4	0.5766	0.6928	0.6776	0.2997	0.6853	0.6525
7	5	1.633	2	0.1682	0.3466	0.2552	0.1297	0.3466	0.2551
			3	0.1588	0.3723	0.2374	0.1152	0.3723	0.2374
			4	0.1515	0.3931	0.2242	0.1047	0.3931	0.2241
11	3	1.967	2	0.7838	0.6629	0.8119	0.4745	0.6576	0.8010
			3	0.7631	0.7188	0.7925	0.4181	0.7119	0.7809
			4	0.7482	0.7576	0.7785	0.3789	0.7497	0.7665
11	5	1.903	2	0.7098	0.5943	0.7552	0.4380	0.5883	0.7469
			3	0.6853	0.6432	0.7314	0.3863	0.6350	0.7234
			4	0.6675	0.6772	0.7142	0.3506	0.6674	0.7063
11	9	1.538	2	0.1003	0.2862	0.1256	6.307×10^{-2}	0.2847	0.1256
			3	9.645×10^{-2}	0.3014	0.1199	5.865×10^{-2}	0.3023	0.1199
			4	9.317×10^{-2}	0.3144	0.1152	5.509×10^{-2}	0.3170	0.1152

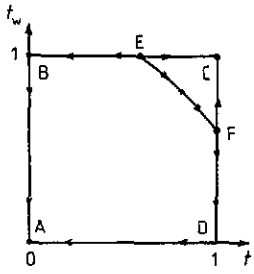

Figure 5. Phase diagram for a Sierpinski carpet with a scattered cut-out: $b = 7$, $l = 3$ (cf figure 1(b)).

These relations have been obtained for the case $l = (b - 1)/2$. The qualitative phase diagram obtained in the low lacunarity case is shown in figure 5. Although this figure was calculated for $b = 7$ and $l = 3$, which has the same values as figure 4(c), the fixed point F now lies on the $t = 1$ axis. An analysis similar to that presented for large-lacunarity carpets, together with numerical calculations, yields table 4. We note the variation in the critical exponents when we keep D constant and vary L. Thus the exponent ν^F increases as L decreases.

For the Potts model in the presence of a bond inhomogeneity, t and t_w are independent random variables distributed according to the following probability laws:

$$\mathcal{P}(t) = (1 - p)\delta(t) + p\delta(t - t_0) \tag{4.6}$$

$$\mathcal{P}(t_w) = (1 - p_w)\delta(t_w) + p_w\delta(t_w - t_{w,0}) \tag{4.7}$$

where p and p_w are the bond concentrations for t and t_w, respectively. The renor-

Table 4. Results for the Potts model on Sierpinski carpets where L was calculated according to (2.2) and (2.3).

b	l	D	L	q	t^E	y_T^E	t^F	t_w^E	y_T^E	t_c
7	3	1.896	3.9377	2	0.6267	0.6015	0.7254	0.3865	0.5988	0.7013
				3	0.5976	0.6552	0.6977	0.3346	0.6497	0.6729
				4	0.5766	0.6928	0.6776	0.2997	0.6853	0.6525
7	3	1.896	0.9984	2	0.5675	0.5922	1	0.6031	0.4504	0.8006
				3	0.5391	0.6480	1	0.5675	0.4931	0.7753
				4	0.5186	0.6878	1	0.5420	0.5231	0.7570
11	5	1.903	24.039	2	0.7098	0.5943	0.7552	0.4380	0.5883	0.7469
				3	0.6853	0.6432	0.7314	0.3863	0.6350	0.7234
				4	0.6675	0.6772	0.7142	0.3506	0.6674	0.7063
11	5	1.903	3.9006	2	0.6519	0.5960	1	0.6998	0.4987	0.8470
				3	0.6275	0.6491	1	0.6701	0.5452	0.8283
				4	0.6098	0.6867	1	0.6488	0.5781	0.8148

malization procedure transforms $\mathcal{P}(t)$ and $\mathcal{P}(t_w)$ into $\mathcal{P}'(t')$ and $\mathcal{P}'(t'_w)$ which are of more complicated forms than the initial distributions. We approximate the transformed distributions by those having the initial forms

$$\mathcal{P}'_{\text{approx}}(t') = (1 - p')\delta(t') + p'\delta(t' - t'_0) \tag{4.8}$$

$$\mathcal{P}'_{\text{approx}}(t'_w) = (1 - p'_w)\delta(t'_w) + p'_w\delta(t'_w - t'_{w,0}). \tag{4.9}$$

This enables us to obtain the recursion relations for the variables p, p_w, t and t_w. For the case $b = 3, l = 1$ the recursion relations are

$$p' = 1 - (1 - p^3)(1 - p^2 p_w)^2 \tag{4.10}$$

$$p'_w = 1 - (1 - p_w^3)(1 - p^2 p_w) \tag{4.11}$$

$$\begin{aligned} p't' = {} & p^7 p_w^2 f[f^{-1}(t^3) + 2f^{-1}(t^2 t_w)] + p^4 p_w^2 (1 - p^3) f[2f^{-1}(t^2 t_w)] \\ & + 2p^5 p_w (1 - p^2 p_w) f[f^{-1}(t^3) + f^{-1}(t^2 t_w)] \\ & + 2p^2 p_w (1 - p^3)(1 - p^2 p_w) f[f^{-1}(t^2 t_w)] \\ & + p^3 (1 - p^2 p_w) f[f^{-1}(t^3)] \end{aligned} \tag{4.12}$$

$$\begin{aligned} p'_w t'_w = {} & p^2 p_w^4 f[f^{-1}(t_w^3) + f^{-1}(t^2 t_w)] + p^2 p_w (1 - p_w^3) f[f^{-1}(t^2 t_w)] \\ & + p_w^3 (1 - p^2 p_w) f[f^{-1}(t_w^3)] \end{aligned} \tag{4.13}$$

where we have dropped the subscript 0 for simplification.

Flows in a four-dimensional parameter space are not easy to visualize. To get a better understanding we shall consider some special subspaces.

(i) Subspace $p = 1, p_w = 1$. This corresponds to the pure system.

(ii) Subspace $t = 1, t_w = 1$. The recursion relations (4.12) and (4.13) reduce, in this case, to (4.10) and (4.11) which describe the percolation behaviour. The same effect is

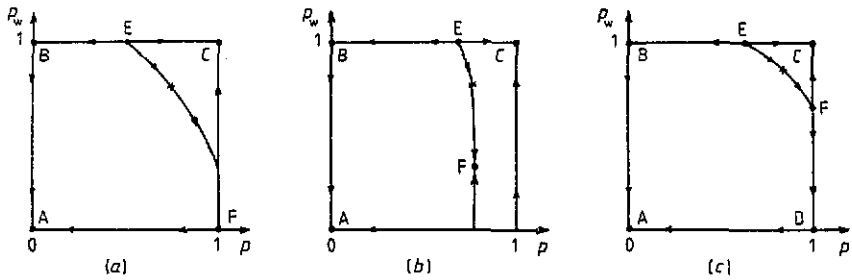

Figure 6. Phase diagrams in the (p, p_w)-space: (*a*) $b = 3$, $l = 1$; (*b*) $b = 7$, $l = 3$ (large lacunarity); (*c*) $b = 7$, $l = 3$ (small lacunarity).

Table 5. Fixed points and critical exponents characterizing bond percolation behaviour in the (p, p_w)-space.

L	b	l	Fixed points		Critical exponents	$p_c = p = p_w$
			(E)	$p = 0.4893$ $p_w = 1$	$y_P = 0.4987$	
Large	3	1				$p_c = 0.7508$
			(F)	$p = 1$ $p_w = 0$	$y_P = 1$	
			(E)	$p = 0.6740$ $p_w = 1$	$y_P = 0.5101$	
Large	7	3				$p_c = 0.7480$
			(F)	$p = 0.7699$ $p_w = 0.4795$	$y_P = 0.4891$	
			(E)	$p = 0.6136$ $p_w = 1$	$y_P = 0.5001$	
Small	7	3				$p_c = 0.8420$
			(F)	$p = 1$ $p_w = 0.6618$	$y_P = 0.3783$	

found for $b \approx 7$ and $l = 3$, for both large- and small-lacunarity families. The corresponding flow diagrams represented in figure 6 show a striking similarity to those of the pure system (figures 4 and 5). There are two non-trivial fixed points characterizing the percolation behaviour whose coordinates and corresponding critical exponents are given in table 5. When $b = 7$ and $l = 3$, for example, the small- and large-lacunarity cases are described by different bond percolation fixed points p_c and different eigenvalue exponents y_p. We note also their variation, when we keep D constant and vary L, similar to that of t_c and y_T for the pure system.

(iii) Subspace $p = p_w$. In this case, bond concentrations for t and t_w are equal. As $p = 1$ is an invariant subspace, the t- and t_w-coordinates of the two non-trivial fixed points listed in tables 3 and 4 are not modified. The coordinates and critical exponents of the new fixed points characterizing the percolation behaviour are listed in table 6 for the case $b = 3$ and $l = 1$. The qualitative phase diagram in the (t, t_w, p)-space, given by the recursion relations (4.10)–(4.13), is represented in figure 7. We find that the fixed points

Table 6. Fixed points and critical exponents characterizing bond percolation behaviour in the (t, t_w, p)-space for $b = 3$ and $l = 1$.

b	l	Fixed points		Critical exponents
3	1	(G)	$t = 0$ $t_w = 0$ $p = 0.6823$	$y_p = 0.6082$
		(H)	$t = 1$ $t_w = 1$ $p = 0.6823$	$y_p = 0.6082$

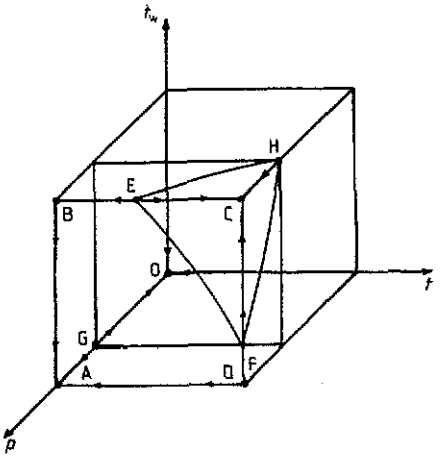

Figure 7. Phase diagram in the (t, t_w, p)-space for $b = 3$ and $l = 1$.

F and G of coordinates $(t^F, t_w^F, 1)$ and $(0, 0, p^G)$ characterize two transition surfaces. At a point of these surfaces the system exhibits a transition between the phases C(1, 1, 1), O(0, 0, 0) and A(0, 0, 1), O(0, 0, 0), respectively. The fixed points $E(t^E, 1, 1)$ and $H(1, 1, p^H)$ represent transition lines at $t_w = 1$ and $t = 1$, respectively.

5. Conclusion

We have performed a renormalization group analysis for a dilute Potts model on Sierpinski carpets. We have investigated the influence of bond dilution on the phase diagrams and we have calculated the dependence of the critical exponents upon fractal dimension and lacunarity. We found that the diluted system and percolation behaviour is characterized by a bond percolation fixed point and its associated eigenvalue exponent, whose variation with fractal geometries is similar to that of the critical temperature and thermal exponent shown previously for both the Ising and the Potts models.

Acknowledgments

One of the authors (A Bakchich) would like to thank Professor Abdus Salam, International Atomic Energy Agency, and UNESCO for hospitality at the International Centre for Theoretical Physics, Trieste, Italy, where this work was completed.

References

Berker A N and Kadanoff L P 1980 *J. Phys. A: Math. Gen.* **13** L259
Bhanot G, Duke D and Salvador R 1985 *Phys. Lett.* **165B** 355
Bhanot G, Neuberger H and Shapiro J A 1984 *Phys. Rev. Lett.* **53** 2277
Boccara N and Havlin S 1984 *J. Phys. A: Math. Gen.* **17** L547
Bonnier B, Leroyer Y and Meyers C 1987 *J. Physique* **48** 553
Dhar D 1977 *J. Math. Phys.* **18** 577
—— 1988 *J. Physique* **49** 397
Gefen Y, Aharony A and Mandelbrot B B 1984 *J. Phys. A: Math. Gen.* **17** 1277
Gefen Y, Mandelbrot B B and Aharony A 1980 *Phys. Rev. Lett.* **45** 855
Gefen Y, Meir Y, Mandelbrot B B and Aharony A 1983 *Phys. Rev. Lett.* **50** 145
Hao L and Yang Z R 1987 *J. Phys. A: Math. Gen.* **20** 1627
Hu B 1985 *Phys. Rev. Lett.* **55** 2316
Kadanoff L P 1976 *Ann. Phys., NY* **100** 359
Lin B and Yang Z R 1986 *J. Phys. A: Math. Gen.* **19** L49
Melrose J R 1983 *J. Phys. A: Math. Gen.* **16** 3077
Migdal A A 1975 *Zh. Eksp. Teor. Fiz.* **69** 810 (Engl. Transl. 1975 *Sov. Phys.–JETP* **42** 743)
Nelson D R and Fisher M E 1975 *Ann. Phys., NY* **91** 226
Riera R and Chaves C M 1986 *Z. Phys.* B **62** 387
Stinchcombe R B 1983 *Phase Transitions and Critical Phenomena* vol 7, ed C Domb and J L Lebowitz (New York: Academic)
Taguchi Y 1987 *J. Phys. A: Math. Gen.* **20** 6611
Wilson K G and Fisher M E 1972 *Phys. Rev. Lett.* **28** 240
Wu F Y 1980 *J. Stat. Phys.* **23** 773
Wu Y K 1988 *J. Phys. A: Math. Gen.* **21** 4251
Wu Y K and Hu B 1987 *Phys. Rev.* A **35** 1404